BJ www.biochemj.org

BJ Disease

Biochem. J. (2009) **421**, 17–27 (Printed in Great Britain) doi:10.1042/BJ20082429

Group III secreted phospholipase A_2 transgenic mice spontaneously develop inflammation

Hiroyasu SATO*†, Yoshitaka TAKETOMI*‡, Yuki ISOGAI*§, Seiko MASUDA*†, Tetsuyuki KOBAYASHI§, Kei YAMAMOTO* and Makoto MURAKAMI*‖[1]

*Biomembrane Signaling Project, The Tokyo Metropolitan Institute of Medical Science, 3-18-22 Honkomagome, Bunkyo-ku, Tokyo 113-8613, Japan, †Department of Health Chemistry, School of Pharmaceutical Sciences, Showa University, 1-5-8 Hatanodai, Shinagawa-ku, Tokyo 142-8555, Japan, ‡Center for Biotechnology, Showa University, 1-5-8 Hatanodai, Shinagawa-ku, Tokyo 142-8555, Japan, §Department of Biological Sciences, Graduate School of Humanities and Sciences, Ochanomizu University, 2-1-1 Ohtsuka, Bunkyo-Ku, Tokyo 112-8610, Japan, and ‖PRESTO, Japan Science and Technology Agency, 4-1-8 Honcho Kawaguchi, Saitama 332-0012, Japan

PLA_2 (phospholipase A_2) group III is an atypical $sPLA_2$ (secretory PLA_2) that is homologous with bee venom PLA_2 rather than with other mammalian $sPLA_2$s. In the present paper, we show that endogenous group III $sPLA_2$ (PLA2G3) is expressed in mouse skin and that Tg (transgenic) mice overexpressing human PLA2G3 spontaneously develop skin inflammation. *Pla2g3*-Tg mice over 9 months of age frequently developed dermatitis with hyperkeratosis, acanthosis, parakeratosis, erosion, ulcer and sebaceous gland hyperplasia. The dermatitis was accompanied by infiltration of neutrophils and macrophages and by elevated levels of pro-inflammatory cytokines, chemokines and prostaglandin E_2. In addition, *Pla2g3*-Tg mice had increased lymph aggregates and mucus in the airway, lymphocytic sialadenitis, hepatic extramedullary haemopoiesis, splenomegaly with increased populations of granulocytes and monocytes/macrophages, and increased serum IgG_1. Collectively, these observations provide the first demonstration of spontaneous development of inflammation in mice with Tg overexpression of mammalian $sPLA_2$.

Key words: dermatitis, phospholipase A_2, phospholipid, prostaglandin, splenomegaly, transgenic mouse.

INTRODUCTION

PLA_2 (phospholipase A_2) enzymes catalyse the hydrolysis of the *sn*-2 position of glycerophospholipids to give rise to fatty acids and lysophospholipids. They are subdivided into several groups: high-molecular-mass intracellular PLA_2s with a catalytic serine residue, including $cPLA_2$ (cytosolic PLA_2) and $iPLA_2$ (Ca^{2+}-independent PLA_2) enzymes, and low-molecular-mass disulfide-rich Ca^{2+}-dependent $sPLA_2$ (secretory PLA_2) family with a catalytic histidine residue. To date, ten catalytically active $sPLA_2$ enzymes have been identified in mammals (IB, IIA, IIC, IID, IIE, IIF, III, V, X and XIIA). On a structural basis, these enzymes are subdivided further into three branches, namely group I/II/V/X, group III and group XII [1–3]. Individual $sPLA_2$s exhibit unique tissue and cellular localizations and enzymatic properties, suggesting their distinct tissue-specific roles in various pathophysiological events.

Because group IIA $sPLA_2$ (PLA2G2A; or synovial $sPLA_2$) is strongly induced during inflammatory conditions such as rheumatoid arthritis or sepsis and because $sPLA_2$s from snake or bee venom can elicit inflammation when administered *in vivo*, it has long been thought that $sPLA_2$ contributes to inflammation, probably by augmenting the generation of pro-inflammatory lipid mediators [1–3]. However, Tg (transgenic) mice overexpressing PLA2G2A do not show any sign of inflammation, even though they have alopecic skin [4], raising the question as to whether this $sPLA_2$ actually exerts a pro-inflammatory role *in vivo*. Although recent gene targeting studies of new members of the $sPLA_2$ family, group V (PLA2G5) and group X (PLA2G10), have provided several lines of evidence that they participate in some types of inflammation [5–8], general understanding of the roles played by $sPLA_2$s in the onset of inflammation, including their modes of action, is still incomplete and needs further clarification. Nonetheless, Tg strategies are still likely to provide some functional and mechanistic insights into the *in vivo* actions of $sPLA_2$s, as knowledge of the antibacterial and pro-atherogenic properties of $sPLA_2$s has been advanced by studies using *Pla2g2a*-Tg mice [9,10]. However, the early mortality of *Pla2g5*-Tg mice [11] and macrophage-specific *Pla2g10*-Tg mice [12] due to lung injury probably resulting from aberrant surfactant degradation limits their subsequent use. So far, there has been no $sPLA_2$-Tg mouse model that spontaneously develops systemic inflammation.

Group III $sPLA_2$ (PLA2G3) is unique in that it consists of a central $sPLA_2$ (S) domain, which is homologous with bee venom $sPLA_2$ rather than with other mammalian $sPLA_2$s, flanked by distinctive N- and C-terminal domains [13]. Forced expression of PLA2G3 or its central S domain alone in several cell types results in increased arachidonic acid metabolism, for which its potency is superior to that of PLA2G2A and next to that of PLA2G10 and PLA2G5 [14,15]. In an effort to elucidate the functions of PLA2G3 *in vivo*, we have recently generated Tg mice expressing human PLA2G3 in all tissues under the control of the CAG (chicken β-actin) promoter. An initial study of *Pla2g3*-Tg mice provided the novel information that PLA2G3 can hydrolyse PC (phosphatidylcholine) in plasma lipoproteins to facilitate macrophage foam cell formation *ex vivo* and atherosclerosis

Abbreviations used: BRAK, breast- and kidney-expressed chemokine; CAG, chicken β-actin; COX, cyclo-oxygenase; ESI, electrospray ionization; GAPDH, glyceraldehyde-3-phosphate dehydrogenase; HDC, histidine decarboxylase; HDL, high-density lipoprotein; IFN, interferon; IL, interleukin; LDL, low-density lipoprotein; LNL, LoxP–neomycin-resistance gene–LoxP; LPS, lipopolysaccharide; LTB_4, leukotriene B_4; MCP-1, monocyte chemoattractant protein-1; mMCP, mouse mast cell protease; mPGES, microsomal prostaglandin E synthase; MPO, myeloperoxidase; NK, natural killer; PAF, platelet-activating factor; PAS, periodic acid–Schiff; PC, phosphatidylcholine; PGE_2, prostaglandin E_2; PLA_2, phospholipase A_2; $cPLA_2$, cytosolic PLA_2; $sPLA_2$, secretory PLA_2; PLA2G2A (etc.), $sPLA_2$ group IIA (etc.); RT, reverse transcription; Tg, transgenic; TNFα, tumour necrosis factor α; WT, wild-type.

[1] To whom correspondence should be addressed (email murakami-mk@igakuken.or.jp).

in vivo [16]. In the present study, we have demonstrated another aspect of *Pla2g3*-Tg mice in that they spontaneously develop inflammation in multiple organs as they age. This mouse model will therefore be useful for analysing and understanding the molecular events in inflammation caused by increased expression of $sPLA_2$.

MATERIALS AND METHODS

Animals

All mice were housed in climate-controlled (21 °C) specific pathogen-free facilities with a 12 h light/12 h dark cycle, with free access to standard laboratory food (Picolab mouse diet 20; Laboratory Diet) and water. All procedures involving animals were performed in accordance with protocols approved by the Institutional Animal Care and Use Committee of Showa University, in accordance with the Standards Relating to the Care and Management of Experimental Animals in Japan. The generation of *Pla2g3*-Tg mice has been reported previously [16].

RT (reverse transcription)–PCR

Total RNA was extracted from mouse tissues with TRIzol® reagent (Invitrogen). For RT–PCR, first-strand cDNA synthesis was carried out using SuperScript III reverse transcriptase kit (Invitrogen). Total RNA (5 μg) was used in reactions primed with oligo(dT) (12–18-mer) primer (Invitrogen) to obtain cDNA. Then, 1 μl of the synthesized cDNA was used as the template for the mRNA-amplification reactions. The PCR amplification was performed on a GeneAmp9600 PCR system (PerkinElmer) with an ExTaq kit (TaKaRa Bio). The primers used are as follows: 5′-GAAAGCATGATCCGCGACGTGGAA-3′ and 5′-CCCTTCTCCAGCTGGAAGACTCCT-3′ for mouse TNFα (tumour necrosis factor α); 5′-AGGGCTGCTTCCAAACCTTTGACC-3′ and 5′-CCAGTTGGGGAACTCTGCAGACTC-3′ for mouse IL (interleukin)-1β; 5′-CAGAGGATACCACTCCCAACAGAC-3′ and 5′-CCTTAGCCACTCCTTCTGTGACTC-3′ for mouse IL-6; 5′-CAGCTAGTTGTCATCCTGCTCTTC-3′ and 5′-GGTGCAGCTTATCGATGAATCCAG-3′ for mouse IL-4; 5′-GCTACACACTGCATCTTGGCTTTG-3′ and 5′-GTGGGTTGTTGACCTCAAACTTGG-3′ for mouse IFNγ (interferon γ); 5′-CGTGCACTGAGGCTCACAAATGTTTC-3′ and 5′-TTTCTTGCACCAGCCATGAGC-3′ for mouse IL-12 p40 subunit; 5′-CATGCTTCTGGGCCTGCTGTTC-3′ and 5′-CAGAAGTGCTTGAGGTGGTTGTGG-3′ for mouse CCL2/MCP-1 (monocyte chemoattractant protein-1); 5′-AAGGGGCCCAAGATCCGCTACA-3′ and 5′-GTAGACCCTGCGCTTCTCGTTCCA-3′ for mouse CXCL14/BRAK (breast- and kidney-expressed chemokine); 5′-GAGCACTGGCCACTCTTCAGAGTCAG-3′ and 5′-CGAGGAGTTCCCAGCAGAATCTCCAA-3′ for human PLA2G3; 5′-GGCTGAGGCCACCTCATATACTTC-3′ and 5′-TCCTTTGCCCTCAGCACAGTCAAG-3′ for mouse PLA2G3; 5′-GGTCTCCTCACACTGGCTTGGTTC-3′ and 5′-CAGTAGACCAGCTTCCGGTCACAG-3′ for mouse PLA2G5; 5′-GACCCGGATTCAGCGAAGCAACCA-3′ and 5′-CAGCTCCTCGTCACACCTGCACAA-3′ for mouse PLA2G10; 5′-GCTGGCCGGTATAACTGCAA-3′ and 5′-ACACAGTTGCCTTTCACACCA-3′ for mouse PLA2G2D; 5′-ACCTCCCATTGCCCTGGCTT-3′ and 5′- GGCCCAGTACACAGCTTGTTGG-3′ for mouse PLA2G2E; 5′-GGTTAAACACTCCACTGGACGGAA-3′ and 5′-CTCGGTACTTGTTCCTGTATGGGT-3′ for mouse PLA2G2F; 5′-CGCTCCATTAAGCTGTGGTTTGTGATTCGG-3′ and 5′-AGACTGGCTCCTGGCTGCTTGATGATCTTC-3′ for mouse HDC (histidine decarboxylase); 5′-ACCACATTCTCGCCCTTACAT-3′ and 5′-TCTCAGTTTCACCTCCCTCAG-3′ for mMCP (mouse mast cell protease)-4; 5′-ATAACAGTCCTCCTAGGAGCC-3′ and 5′-GATCCAGGGCCTGTAATGGGA-3′ for mMCP-5; 5′-GCACATCAAAAGCCCACAGC-3′ and 5′-TAGACAGGGGAGACAGAGGAC-3′ for mMCP-6; and 5′-TCGTGGATCTGACGTGCCGCCTG-3′ and 5′-CACCACCCTGTTGCTGTAGCCGTAT-3′ for mouse GAPDH (glyceraldehyde-3-phosphate dehydrogenase). The PCR products were analysed on a 1.5 % agarose gel and visualized using ethidium bromide staining.

Quantitative RT–PCR

For quantitative RT–PCR, cDNA synthesis was performed using the high-capacity cDNA reverse transcription kit (Applied Biosystems). The reaction was carried out on an ABI Prism 7000 sequence detection system (Applied Biosystems) with TaqMan gene expression master mix (Applied Biosystems). Pre-designed TaqMan assays (Applied Biosystems) were used to determine gene expression: Mm00839636 for mouse CD68, Mm00478374 and Mm00478374 for mouse COX (cyclooxygenase)-1 and -2 respectively, Mm00447040 for mouse $cPLA_2\alpha$, and Mm00452105 and Mm00460181 for mouse mPGES (microsomal prostaglandin E synthase)-1 and -2 respectively.

Histochemistry

Formalin-fixed tissues were embedded in paraffin, sectioned, mounted on glass slides, deparaffinized in xylene and rehydrated in ethanol with increasing concentrations of water. The cell type was identified from conventional haematoxylin and eosin staining. For PAS (periodic acid–Schiff) staining, tissue sections were deparaffinized, rehydrated and placed in 0.5 % periodic acid solution for 5 min. After washing in water, the sections were placed in Coleman's Schiff reagent for 15 min, washed in water for 10 min and counterstained with haematoxylin solution for 15 min. After washing in water for 15 min, the sections were dehydrated and mounted with resinous medium.

Measurement of eicosanoids

The contents of PGE_2 (prostaglandin E_2) and LTB_4 (leukotriene B_4) in mouse skins were quantified using PGE_2 and LTB_4 enzyme immunoassay kits (Cayman Chemicals).

Measurement of MPO (myeloperoxidase) activity

The tissue samples were homogenized in 50 mM potassium phosphate buffer (pH 6.0) containing 1 % (w/v) hexadecyltrimethylammonium bromide and centrifuged at 12000 ***g*** for 15 min at 4 °C. An aliquot (30 μl) was added to 180 μl of the buffer containing 0.167 mg/ml *o*-dianisidine dihydrochloride and 0.0005 % (v/v) hydrogen peroxidase (Sigma–Aldrich). After appropriate periods of incubation at 37 °C, the absorbance at 460 nm was measured. MPO activity was calculated using a standard curve generated with human MPO (Sigma), and values were normalized to protein concentration.

Determination of cell types in blood circulation

Blood was collected from mouse tail biopsy with 10 mM EDTA as an anticoagulant. The blood samples were applied to a clinical blood cell analyser VetScan HM (Abaxis) to determine the numbers of lymphocytes, granulocytes, monocytes, erythrocytes and platelets, the haemoglobin content and the haematocrit value.

Flow cytometry (FACS)

Suspensions of 10^6 splenic cells were treated on ice with anti-[mouse CD16/CD32 (FcγRII/RIII)] monoclonal antibody (BD Biosciences) to block cell-surface Fcγ receptors. Then the cells were incubated with FITC-, phycoerythrin- or Alexa Fluor® 488-labelled monoclonal antibodies against mouse CD3, CD4, CD8, CD11b (Mac1), CD11c, CD21, CD23, CD45R, Gr-1, NK1.1, sIgD and sIgM (BD Biosciences). Flow cytometric analysis was carried out on a FACS Aria cell-sorting system (BD Biosciences).

ESI (electrospray ionization)–MS

Lungs of mice were lavaged with 1 ml of SET buffer (250 mM sucrose, 0.5 mM EDTA and 20 mM Tris/HCl, pH 7.4), and the resulting bronchoalveolar lavage fluid was used after centrifugation at 160 ***g*** for 10 min at 4 °C to remove the cells and tissue debris. Lipids were extracted from the bronchoalveolar lavage fluid using the method of Bligh and Dyer [16a]. PC with $C_{14:1}$–$C_{14:1}$ (diacyl) was added to the samples (1 nmol of internal standard per 1 mg of protein equivalents) as an internal standard. MS spectra were obtained on a Quattro Micro tandem quadrupole mass spectrometer (Micromass) equipped with ESI, as described previously [11]. Lipid extracts were reconstituted in 2:1 chloroform/methanol (100–300 μmol of phosphorus/l), and 2 μl of the sample was injected per run. The samples were introduced by means of a flow injector into the ESI chamber at a flow rate of 4 μl/min in a solvent system of acetonitrile/methanol/water (2:3:1, by vol.) containing 0.1 % (v/v) ammonium formate (pH 6.4). The mass spectrometer was operated in the positive- and negative-scan modes. The flow rate of the nitrogen drying gas was 12 l/min at 80 °C. The capillary and cone voltages were set at 3.7 kV and 30 V respectively, argon at $(3–4)\times10^4$ Torr (1 Torr = 133.3 Pa) was used as the collision gas, and a collision energy of 30–40 V was used for obtaining fragment ions for precursor ions.

Determination of serum immunogloblin levels

Serum titres of IgM, IgG_1, IgG_2 and IgE were determined using a mouse IgX ELISA quantification kit (Bethyl Laboratories).

RESULTS

Pla2g3-Tg mice develop dermatitis

Pla2g3-Tg mice appeared normal at birth and showed no apparent abnormality up to 9 months of age under our housing conditions (except that the Tg mice had altered plasma lipoproteins, as described in [16]). Subsequently, however, we noted that about one-third of PLA2G3 mice, both male and female, experienced gradual hair loss on their facial, neck and dorsal skin, which subsequently (typically within 2–3 months) developed into focally alopecic lesions that were often filled with pus (Figure 1A). Behaviour suggestive of increasing itching eventually worsened the lesions further. Neither age-matched non-Tg WT (wild-type) mice nor Tg mice expressing LNL (LoxP–neomycin-resistance gene–LoxP)–PLA2G3 (i.e. mice harbouring the PLA2G3 transgene in a silent state [16]) exhibited these skin abnormalities (Figure 1A), implying that the phenotype resulted from Tg overexpression of PLA2G3. Subsequent studies mostly focused on aged (9–12 months) PLA2G3 mice that developed dermatitis, with age-matched WT mice as controls.

Histological examination revealed many abnormalities in the skin of *Pla2g3*-Tg mice (Figure 1B, panels b–i) as compared with the normal appearance of the skin of WT mice (Figure 1B, panel a). *Pla2g3*-Tg mice (1-year-old) showed dense cellularity in the dermis with markedly increased numbers of haematoxylin-stained nuclei, which were mostly ascribed to infiltrating polymorphonuclear neutrophils and macrophages (Figure 1B, panels b–i). *Pla2g3*-Tg mice had thickened epidermis (acanthosis) with dense cornified layers, sebaceous gland hyperplasia and epidermal rete peg formation (downward papillary projection of the epidermis) (Figure 1B, panels b and c). In contrast with hair shafts that emerged straight out of the hair canals in WT mice (Figure 1B, panel a), those in *Pla2g3*-Tg mice often bent over within the canals, probably because highly thickened interfollicular and follicular keratinocyte layers prevented the protrusion of the hair shafts (Figure 1B, panel b). Parakeratosis, which represents unusual retention of nuclei in the outermost cornified layers, was frequently observed in severe lesions in *Pla2g3*-Tg mice (Figure 1B, panels c–e), where the epidermis was focally lost resulting in cutaneous erosion and ulcers with massive neutrophil infiltration (Figure 1B, panels d, e, g and h).

RT–PCR showed that pro-inflammatory cytokines, including TNFα, IL-1β and IL-6, and CCL2/MCP-1 were highly expressed in the inflamed skin lesions of *Pla2g3*-Tg mice, but not in control mice (Figure 2A). CXCL14 (BRAK), a skin chemokine, was faintly detected in WT skin and was also increased in Tg skin. The T_{H2} cytokine IL-4 was weakly, but significantly, detected in Tg, but not WT, skin, whereas the T_{H1} cytokines IFNγ and IL-12 were below the detection limit in both genotypes (Figure 2A). Moreover, MPO activity, which mirrors neutrophil infiltration, in skin sections was markedly elevated in *Pla2g3*-Tg mice compared with WT mice (Figure 2B). Quantitative RT–PCR demonstrated a marked increase in CD68, a macrophage marker, in *Pla2g3*-Tg skin relative to WT skin (Figure 2C), consistent with macrophage infiltration. In contrast, the expression levels of mast cell markers, including mMCP-4, -5 and -6 (mast cell proteases), were unchanged between control and PLA2G3 skin (Figure 2D), indicating that the mast cell population was unaffected by Tg expression of PLA2G3. Therefore increased expression of HDC (a histamine-biosynthetic enzyme) in the Tg skin (Figure 2D) might reflect the increase in macrophages, in which a trace level of HDC is expressed [17], or, alternatively, the expression of HDC, but not mMCPs, in mast cells might be specifically controlled by PLA2G3.

Furthermore, a marked increase in PGE_2 was observed in the skin of *Pla2g3*-Tg mice compared with that of WT mice (Figure 3A). Consistent with this, expression of COX-2 and mPGES-1, which are inducible enzymes that act sequentially in the PGE_2-biosynthetic pathway downstream of PLA_2 [18], was higher in *Pla2g3*-Tg skin lesions than in WT skin (Figure 3B). In particular, the induction of COX-2 was markedly higher in Tg skin relative to WT skin, whereas cutaneous expression levels of cPLA$_2\alpha$, COX-1 and mPGES-2 were similar between the genotypes (Figure 3B). Therefore increased expression of pro-inflammatory cytokines by infiltrating macrophages or hyperplasic epidermal keratinocytes may contribute to the induction of COX-2 and mPGES-1, which in turn leads to increased PGE_2 synthesis in *Pla2g3*-Tg skin. Although we also measured LTB_4, a leukotriene produced by neutrophils and macrophages, in skin homogenates as well as serum of *Pla2g3*-Tg mice, it was below the detection limit probably because of its instability.

The expression of various sPLA$_2$ enzymes in the skin of WT and Tg mice is shown in Figure 3(C). Interestingly, transcripts of endogenous mouse PLA2G3 were clearly detected in control skin (Figure 3C). To our knowledge, this is the first demonstration that PLA2G3 is intrinsically expressed in mouse skin. Expression of PLA2G2D and PLA2G5 was increased in Tg lesion skin

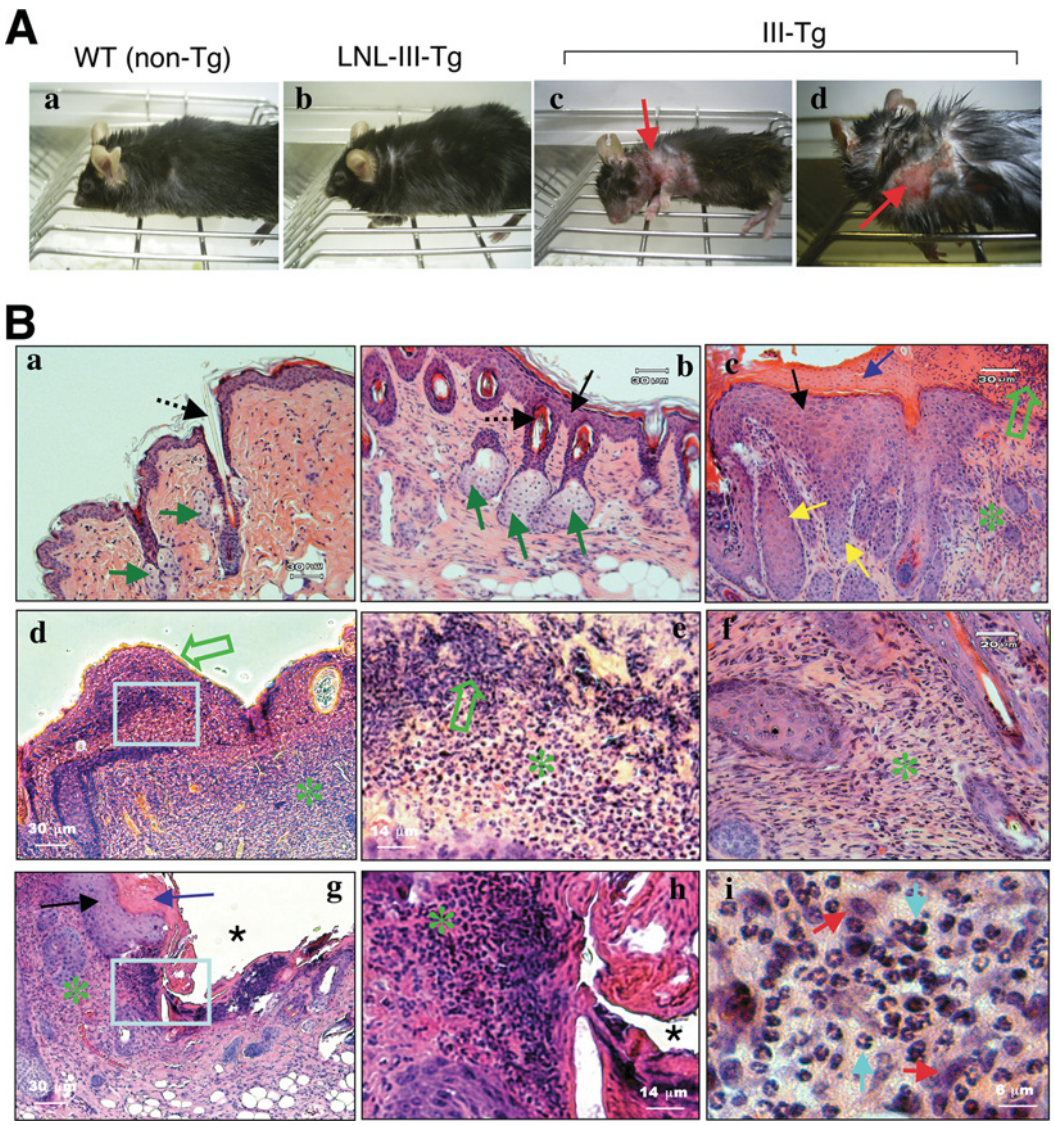

Figure 1 Histology of dermatitis in aged *Pla2g3*-Tg mice

(**A**) Appearance of 1-year-old WT (panel a), *LNL–Pla2g3*-Tg (LNL-III-Tg) (panel b) and *CAG–Pla2g3*-Tg (III-Tg) (panels c and d) mice. Whereas WT and LNL–*Pla2g3*-Tg mice were grossly normal, *CAG–Pla2g3*-Tg mice frequently developed lesion areas on facial, neck and back skins (red arrows). (**B**) Skin histology of WT and *Pla2g3*-Tg mice. In contrast with the normal appearance of the skins of WT mice (panel a), those of *Pla2g3*-Tg mice showed multiple abnormalities (panels b–i) that are similar to those seen in psoriasis and atopic dermatitis in humans. Typically, the Tg skins exhibit hyperkeratosis (dark arrows; panels b, c and g) with thickened cornified layers (blue arrows; panels c and g), acanthosis (yellow arrows; panel c) and parakeratosis (open green arrows; panels c–e). Sebaceous glands (green arrows) are hyperplasic and hair shafts (broken arrows) were bent over within hair follicles in *Pla2g3*-Tg mice (panel b) compared with normal appearance of those in control mice (panel a). Epidermis was focally lost, where erosion and ulcer (stars) were found in the Tg mice (panels d, e, g and h). Boxed areas in panels d and g are magnified in panels e and h respectively. A lot of inflammatory cell infiltrates were found in the dermis of the Tg mice (green asterisks, panels c–h). A magnified vision of the Tg dermis demonstrates the accumulation of polymorph nuclear neutrophils and flat-shaped mononuclear macrophages, as exemplified by light blue arrows and red arrows respectively in panel i.

compared with unaffected Tg skin and with WT skin, whereas expression of PLA2G10 was below the detection limit in the skin of both genotypes (Figure 3C). Another intriguing finding is constitutive expression of PLA2G2E and PLA2G2F at relatively high levels in the skin of both genotypes (Figure 3C).

Inflammation in other tissues

The finding that several inflammatory markers were elevated in the skin lesions of *Pla2g3*-Tg mice (Figures 2 and 3) prompted us to examine whether other tissues in these mice also display inflammatory symptoms. We showed previously that *Pla2g5*-Tg mice die at birth because of lung injury resulting from aberrant hydrolysis of lung surfactant phospholipids, and that the lungs of newborn *Pla2g5*-Tg mice are characterized by abnormally thickened alveolar walls with formation of hyaline membranes lining the alveolar surfaces [11]. In marked contrast, the alveolar architecture of *Pla2g3*-Tg mice was largely indistinguishable from that of age-matched WT mice (Figure 4A, panels a and b). When surfactant lipids were extracted from bronchoalveolar lavage fluid of WT and *Pla2g3*-Tg mice and were subjected to ESI–MS analysis, the composition of the surfactant PC (Figure 4B) and phosphatidylglycerol (results not shown) was similar in WT and *Pla2g3*-Tg mice. However, goblet cell hyperplasia, which was visualized by PAS staining, was evident in the bronchial epithelium of *Pla2g3*-Tg mice compared with

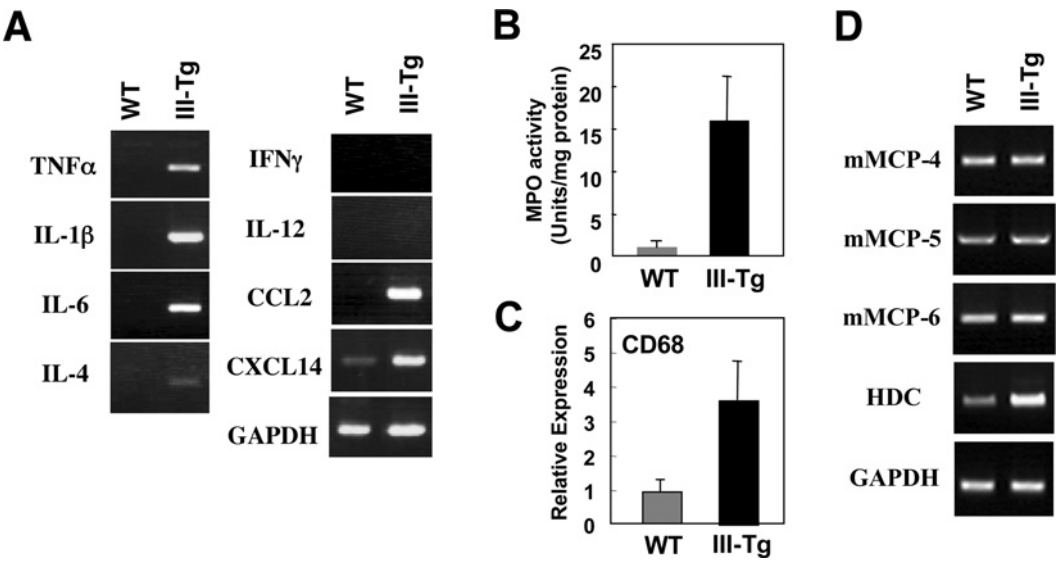

Figure 2 Increases in expression of cytokines/chemokines and infiltration of neutrophils/macrophages in skin of *Pla2g3*-Tg mice

(**A**) RNAs prepared from the skin of WT mice (left-hand lanes) and *Pla2g3*-Tg mice (III-Tg; right-hand lanes) were subjected to RT–PCR to assess the expression of pro-inflammatory (TNFα, IL-1β and IL-6), T_{H2} (IL-4) and T_{H1} (IFNγ and IL-12 p40 subunit) cytokines, and chemokines (CCL2 and CXCL14). RT–PCR for GAPDH was also carried out to verify equal loading of samples into each lane. (**B**) MPO activity in homogenates of WT and *Pla2g3*-Tg (III-Tg) skin (means $\pm$ S.D., $n = 3$). (**C**) Expression of CD68, a macrophage marker, in skin from WT mice and *Pla2g3*-Tg mice (III-Tg) was assessed using quantitative RT–PCR (means $\pm$ S.D., $n = 3$). (**D**) Expression of mMCP-4, -5 and -6 (mast cell proteases) and HDC in WT and Tg skin.

WT mice, suggesting increased mucus secretion in the former (Figure 4A, panels c and d). In addition, perivascular lymph aggregates were frequently found in the lungs of *Pla2g3*-Tg mice compared with WT mice (Figure 4A, panels e and f). These observations suggest that PLA2G3 elicits airway inflammation through a mechanism independent of increased lung surfactant hydrolysis.

We also found notable inflammatory changes in salivary glands (Figure 4C) and liver (Figure 4D) of *Pla2g3*-Tg mice. Compared with WT mice (Figure 4C, panel a), the salivary glands of *Pla2g3*-Tg mice showed marked glandular swelling accompanied by infiltration of lymphocytes in the interstitium (Figure 4C, panels b and c); this histological feature resembles lymphocytic sialadenitis in humans. In addition, foci of extramedullary haemopoiesis, an event that often occurs during systemic inflammation, were found in the liver of *Pla2g3*-Tg mice (Figure 4D, panel b), whereas they were absent from WT mice (Figure 4D, panel a).

Furthermore, *Pla2g3*-Tg mice, even at 5 months of age at which time no skin inflammation was apparent, frequently showed splenomegaly (Figure 5A), such that spleen weight in the Tg mice was markedly increased compared with that in WT mice (Figure 5B). We therefore examined splenic cell populations by FACS analysis using antibodies against cell lineage-specific markers. Figure 5(C) summarizes the results. Essentially, there were no appreciable differences in populations of effector T-cells, including $CD4^+$ and $CD8^+$ T-cells, various differential stages of B-cells, including $CD21^+$, $sIgM^+$, $sIgD^+$ and $CD23^+$ cells, and NK (natural killer) ($NK1.1^+$) cells (Figure 5C). In contrast, splenic Gr-1^+ neutrophils, $CD11b^+$ monocytes/macrophages and $CD11c^+$ dendritic cells were increased >2-fold in *Pla2g3*-Tg mice relative to WT mice (Figure 5C). Therefore PLA2G3 overexpression preferentially affects the haemopoietic, rather than the lymphocytic, lineages of splenic cells at this stage.

In agreement with the above observations, numbers of circulating granulocytes and monocytes were increased in 9–10-month-old *Pla2g3*-Tg mice compared with WT mice, whereas they were similar in young adults (2–3-months-old) of both genotypes (Figure 6A, panels a and b). The number of circulating lymphocytes tended to increase in young, rather than aged, PLA2G3 mice relative to WT mice, although this difference was not statistically significant (Figure 6A, panel c). Platelet and erythrocyte counts were unaffected in *Pla2g3*-Tg mice throughout the experimental periods (Figure 6A, panels d and e). Likewise, haemoglobin levels and haematocrit values in the blood were indistinguishable between the genotypes (Figure 6B). In addition, serum IgG_1 was increased >7-fold in aged *Pla2g3*-Tg mice relative to WT mice, whereas serum IgM, IgG_{2a} and IgE levels were unchanged (Figure 6C).

To examine further the potential contribution of PLA2G3 to the inflammatory response, we examined PGE_2 generation *ex vivo* by peritoneal macrophages derived from *Pla2g3*-Tg and WT mice. Spontaneous production of PGE_2 over 12 h of culture was higher in macrophages from Tg mice than in those from control mice (Figure 6D, panel a). After stimulation of macrophages with LPS (lipopolysaccharide) for 24 h, WT-derived cells showed vigorous production of PGE_2, which was further augmented 3-fold in replicate Tg-derived cells (Figure 6D, panel b). These *ex vivo* experiments agree with our previous observations that PLA2G3 has the capacity to augment arachidonic acid metabolism in various cultured cells when overexpressed [14,15]. Moreover, LPS-stimulated *Pla2g3*-Tg macrophages produced more IL-6 than did replicate WT cells (Figure 6E). Even in the absence of LPS stimulation, IL-6 release was significantly increased in macrophages of *Pla2g3*-Tg mice compared with those of control mice (Figure 6E, inset). Thus overexpression of PLA2G3 enhances the inflammatory response in macrophages.

DISCUSSION

Because of the ability of PLA_2 enzymes to release arachidonic acid (a precursor of various lipid mediators such as prostaglandins and leukotrienes) and lysophospholipids such as lysophosphatidic

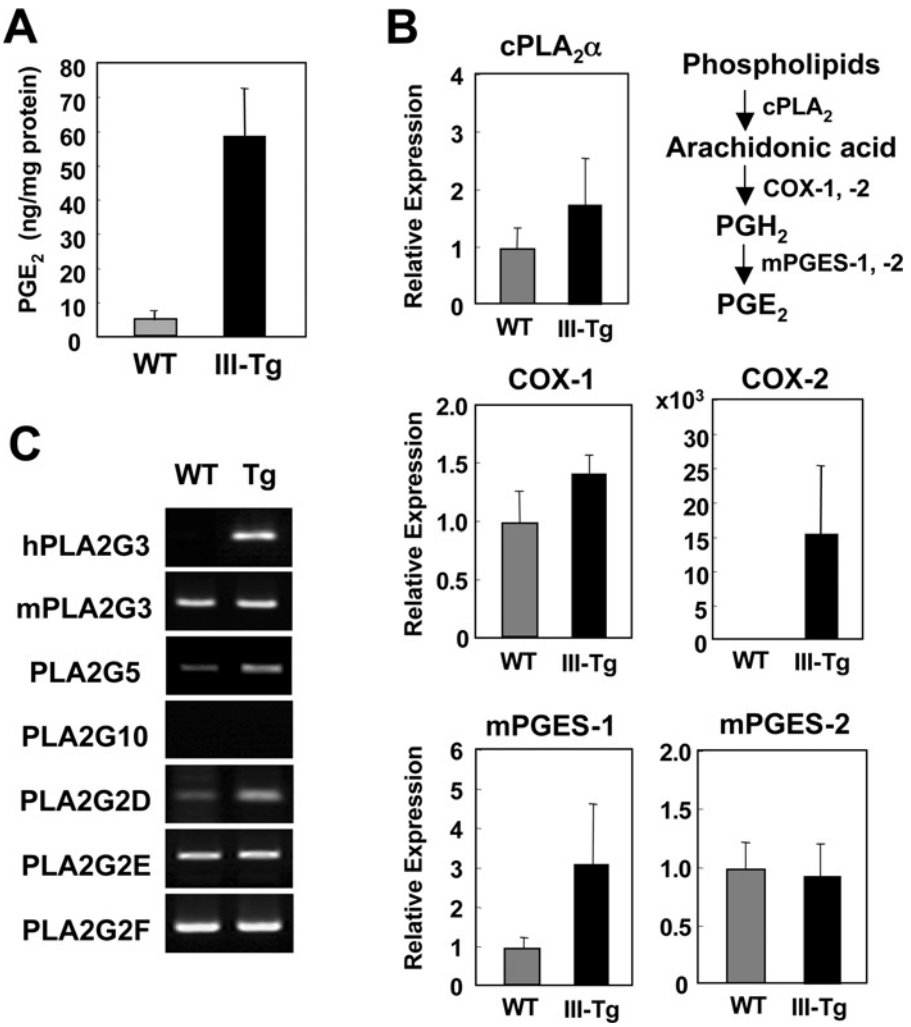

Figure 3 Elevations of PGE_2 and its biosynthetic enzymes in skin of *Pla2g3*-Tg mice

(**A**) Skin homogenates from WT mice and *Pla2g3*-Tg mice (III-Tg) were subjected to PGE_2 enzyme immune assay. (**B**) Expression of PGE_2-biosynthetic enzymes in skins of WT and *Pla2g3*-Tg (III-Tg) mice was assessed by quantitative RT–PCR (means $\pm$ S.D., $n = 3$). The PGE_2-biosynthetic pathway is indicated. PGH_2, prostaglandin H_2. (**C**) Expression of $sPLA_2$s in WT and *Pla2g3*-Tg (Tg) skin was assessed by RT–PCR.

acid and 1-*O*-alkyl lysophosphatidylcholine [a precursor of PAF (platelet-activating factor)] from membrane phospholipids, it has long been thought that these enzymes participate in a wide variety of diseases, such as inflammation, atherosclerosis and cancer, in which lipid mediators play pivotal roles. Gene ablation of group IVA $cPLA_2\alpha$, a stimulus-coupled intracellular PLA_2 that is regulated by phosphorylation and Ca^{2+}-dependent membrane translocation, has established the importance of this arachidonate-selective enzyme in the production of eicosanoids and PAF in most, if not all, cells and tissues [19]. Although several $sPLA_2$s are capable of releasing arachidonic acid from isolated or cultured cells *in vitro* [1–3], the pathophysiological relevance of this event *in vivo* has remained elusive. Although PLA2G2A is a prototypic inflammatory PLA_2 whose expression is markedly elevated during various inflammatory states in humans and experimental animals (except in mice, in which the *Pla2g2a* gene is naturally disrupted (e.g. C57BL/6) or expressed only in the intestine (e.g. BALB/c [20]), its contribution to lipid mediator production *in vivo* has not yet been proven conclusively. Tg mice overexpressing human or mouse PLA2G2A do not show any sign of inflammation, although they display a notable alopecic phenotype with hyperkeratosis [4,21]. Furthermore, animals overexpressing the mouse enzyme are sensitive to two-stage chemical carcinogenesis, with development of a higher number of skin papillomas and then of carcinomas than in replicate control mice [21]. Rather, the main function of PLA2G2A is now recognized to be protection of the host from microbial invasion by degrading bacterial membranes, in which phosphatidylethanolamine and phosphatidylglycerol, two preferred substrates for PLA2G2A, are major phospholipid components [9]. PLA2G5 and PLA2G10 have much higher capacity to interact with PC-rich outer plasma membranes to release arachidonic acid than does PLA2G2A [22,23]. The involvement of both PLA2G5 and PLA2G10 in inflammation and associated lipid-mediator production, such as zymosan-induced peritonitis [5], methacholine-induced airway hypersensitivity [6], T_{H2}-biased asthmatic response [7] and ischaemia/reperfusion-induced myocardial damage [8], has been demonstrated in studies using *Pla2g5*-null or *Pla2g10*-null mice, even though it remains uncertain whether arachidonic acid is supplied directly through the membrane-hydrolytic action of these $sPLA_2$s or indirectly through the activation of $cPLA_2\alpha$ or other enzymes in those situations.

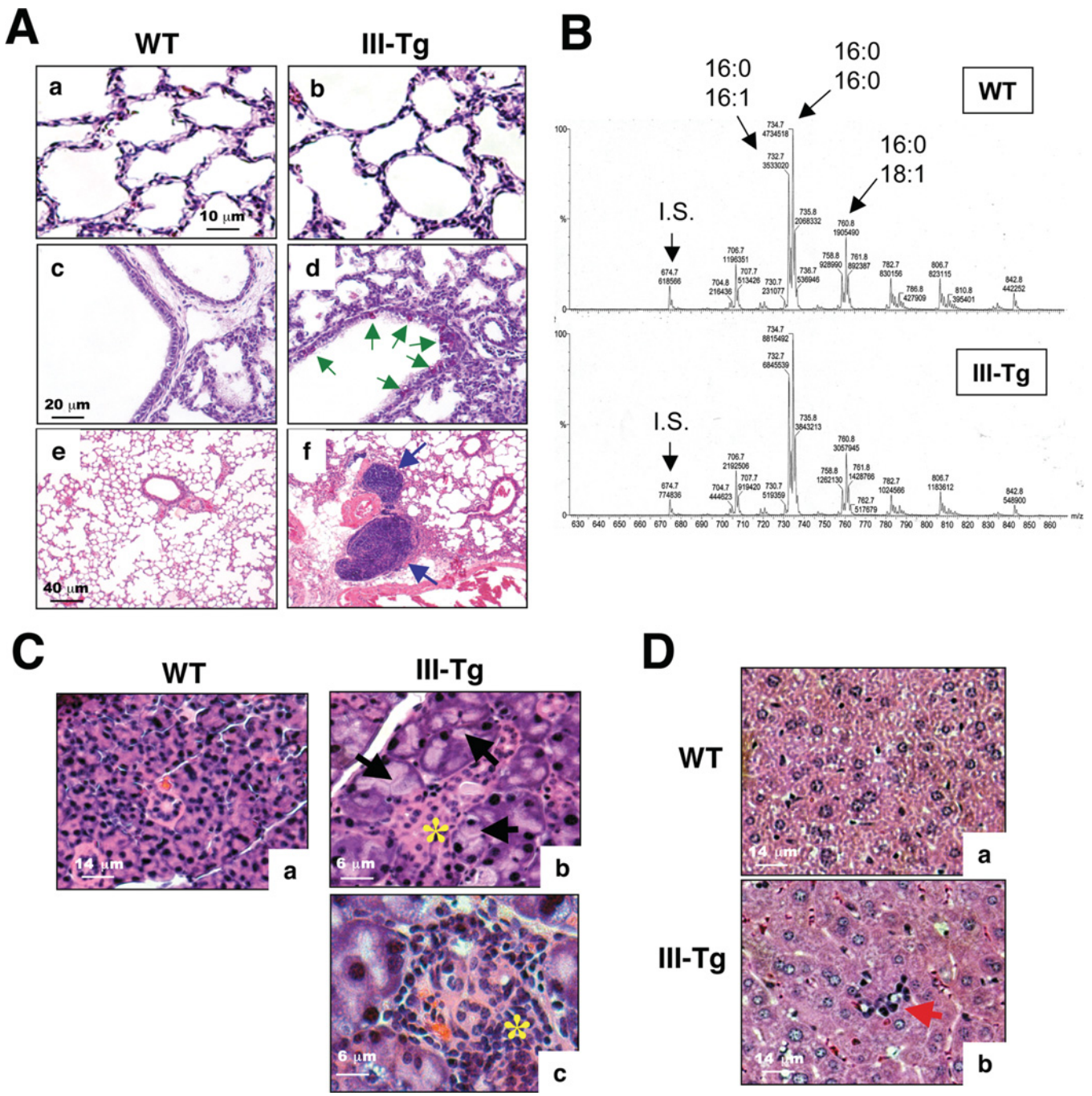

Figure 4 Inflammatory symptoms in multiple tissues of *Pla2g3*-Tg mice

(**A**) Histology of lungs from 1-year-old WT (panels a, c and e) and *Pla2g3*-Tg (III-Tg) mice (panels b, d and f). No overt abnormalities were found in the alveoli of *Pla2g3*-Tg mice (III-Tg; panel b) compared with WT mice (panel c). PAS staining revealed increased goblet cells (green arrows) in the bronchial epithelium of *Pla2g3*-Tg mice (panel d) compared with WT mice (panel c). Perivascular lymph aggregates (blue arrows) were frequently found in the lung of *Pla2g3*-Tg mice (panel f) relative to WT mice (panel e). (**B**) ESI–MS analyses of lung surfactant (PC) prepared from WT mice (upper panel) and *Pla2g3*-Tg mice (III-Tg) (lower panel). Peaks for major PC molecular species and an internal standard (PC with $C_{14:1}$–$C_{14:1}$) are indicated. No abnormality was found in the lung surfactant of *Pla2g3*-Tg mice. I.S., internal standard. (**C**) Histology of salivary glands of 1-year-old WT mice (panel a) and *Pla2g3*-Tg mice (III-Tg; panels b and c). Salivary glands of *Pla2g3*-Tg mice showed glandular swelling (dark arrows) and interstitial lymphocyte infiltration (asterisks). Magnifications, × 200 in panels a and b; × 400 in panel c. (**D**) Histology of livers from 1-year-old WT mice (panel a) and *Pla2g3*-Tg mice (III-Tg; panel b). Extramedullary haemopoiesis was found in the *Pla2g3*-Tg mice (red arrow; panel b). Magnification, × 200.

In the present study, we found that Tg mice carrying the transgene for human PLA2G3, another $sPLA_2$ that is capable of efficient hydrolysis of PC-rich membranes [14,15], frequently developed inflammation as they aged. This is, to our knowledge, the first demonstration that Tg overexpression of a particular form of $sPLA_2$ induces inflammation in the skin. By 1 year of age, *Pla2g3*-Tg mice displayed dermatitis associated with acanthosis, hyperkeratosis, parakeratosis, sebaceous gland hyperplasia, erosion and ulcer, with massive dermal infiltration of inflammatory cells, such as neutrophils and macrophages,

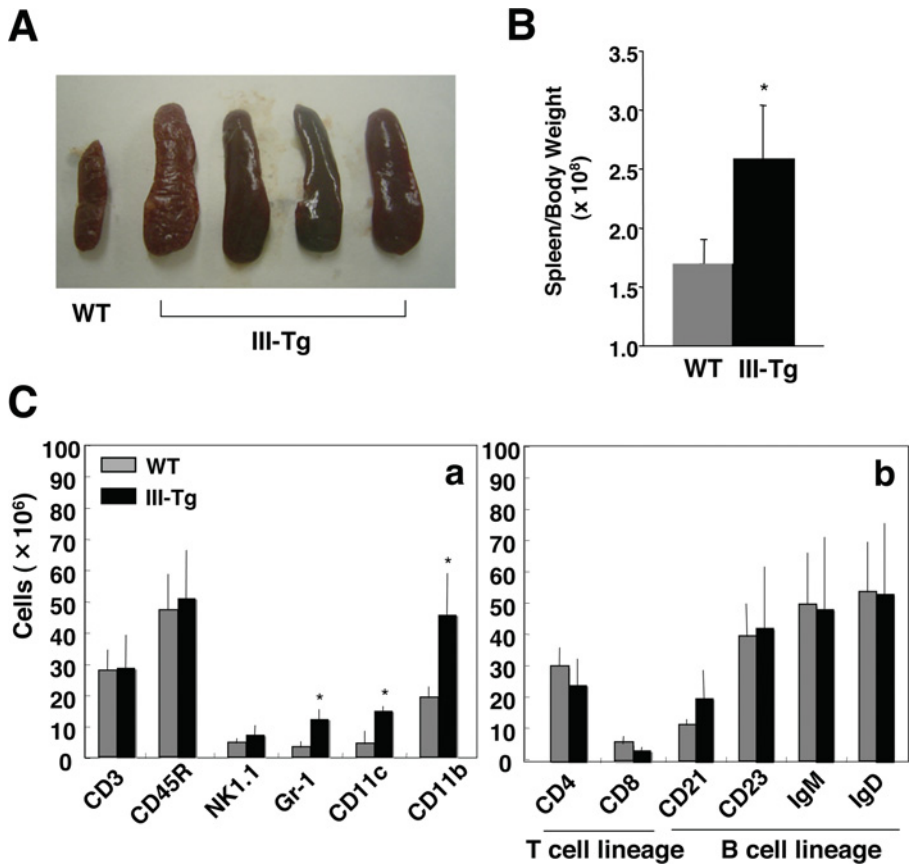

Figure 5 Altered splenic cell populations in *Pla2g3*-Tg mice

(**A**) Splenomegaly of 5-month-old *Pla2g3*-Tg mice (III-Tg) in comparison with that of age-matched WT mice. (**B**) Spleen weight per body weight was nearly doubled in *Pla2g3*-Tg mice (III-Tg) relative to that in WT mice (means ± S.D., $n = 4$, $^*P < 0.05$). (**C**) Distribution of splenic cell populations in WT and *Pla2g3*-Tg (III-Tg) mice. FACS was performed with antibodies for CD3 (T-cells), CD45R (B-cells), NK1.1 (NK cells), Gr-1 (granulocytes), CD11c (dendritic cells) and CD11b (monocytes/macrophages) (left-hand panel). T-cell lineages were sorted further with antibodies for CD4 and CD8, and B-cell lineages were sorted with antibodies for CD21, CD23, sIgM and sIgD (right-hand panel). Values are means ± S.D. for three independent experiments ($^*P < 0.05$).

and elevated expression of pro-inflammatory cytokines and chemokines, such as IL-1β, IL-6, TNFα and CCL2 (Figures 1 and 2). A moderate but significant expression of IL-4, but not IFNγ and IL-12, suggests a tendency to a T_{H2} response rather than a T_{H1} response. The affected skin in *Pla2g3*-Tg mice is histologically similar to that of patients with atopic dermatitis, but is distinct from that of *Pla2g2a*-Tg mice [4], which develop alopecia and epidermal hyperplasia in the absence of inflammation. Therefore the mechanisms underlying the skin phenotypes induced by PLA2G3 (with inflammation) and PLA2G2A (without inflammation) may not be identical.

PGE_2, as well as its biosynthetic enzymes (COX-2 and mPGES-1), was markedly increased in skin lesions of *Pla2g3*-Tg mice (Figure 3), indicating that PLA2G3 facilitates arachidonic acid metabolism. At present, it is unclear whether the elevation of this arachidonate metabolite reflects increased PLA2G3-directed membrane hydrolysis or a secondary effect involving the activation of other PLA_2s (such as cPLA$_2\alpha$) in infiltrating leucocytes, keratinocytes or other cell types in response to elevated levels of pro-inflammatory cytokines/chemokines. Nevertheless, peritoneal macrophages from *Pla2g3*-Tg mice produced more PGE_2 and IL-6 than did those from control mice, particularly after stimulation with LPS (Figures 6D and 6E), an observation that accords with studies showing that PLA2G3 can promote arachidonic acid release in multiple types of cultured cells [14,15] and that the skin lesions in *Pla2g3*-Tg mice showed elevated levels of pro-inflammatory cytokines and PGE_2 with a concomitant infiltration of macrophages (Figures 2 and 3). The inflammatory signs are not restricted to the skin, but are also seen in other tissues including salivary gland, lung, liver, spleen and even blood (Figures 4–6). In this context, a likely explanation for the inflammatory phenotype is that sustained, albeit moderate, increases in levels of lipid mediators within the affected tissues might lead to a gradual onset of inflammation in *Pla2g3*-Tg mice. For instance, PGE_2, through its receptor EP2, promotes epidermal hyperplasia and dermal macrophage infiltration [23a], which are reminiscent of *Pla2g3*-Tg skin (Figure 1). In accordance, episodes of infection with environmental micro-organisms through cutaneous lesions, particularly wounded areas as a result of increasing scratching behaviour, might facilitate the expansion, migration and activation of neutrophils and macrophages, thereby leading to exacerbation of local and systemic inflammatory responses.

It is intriguing to note that the skin inflammation in *Pla2g3*-Tg mice was accompanied by increased expression of PLA2G5 and PLA2G2D (Figure 3C). This suggests that these two sPLA$_2$s are associated with inflammation, either through transcriptional up-regulation in resident cells or through infiltration of inflammatory cells in which these sPLA$_2$s are expressed. Both situations might be applied to PLA2G5, since this enzyme is known to be expressed

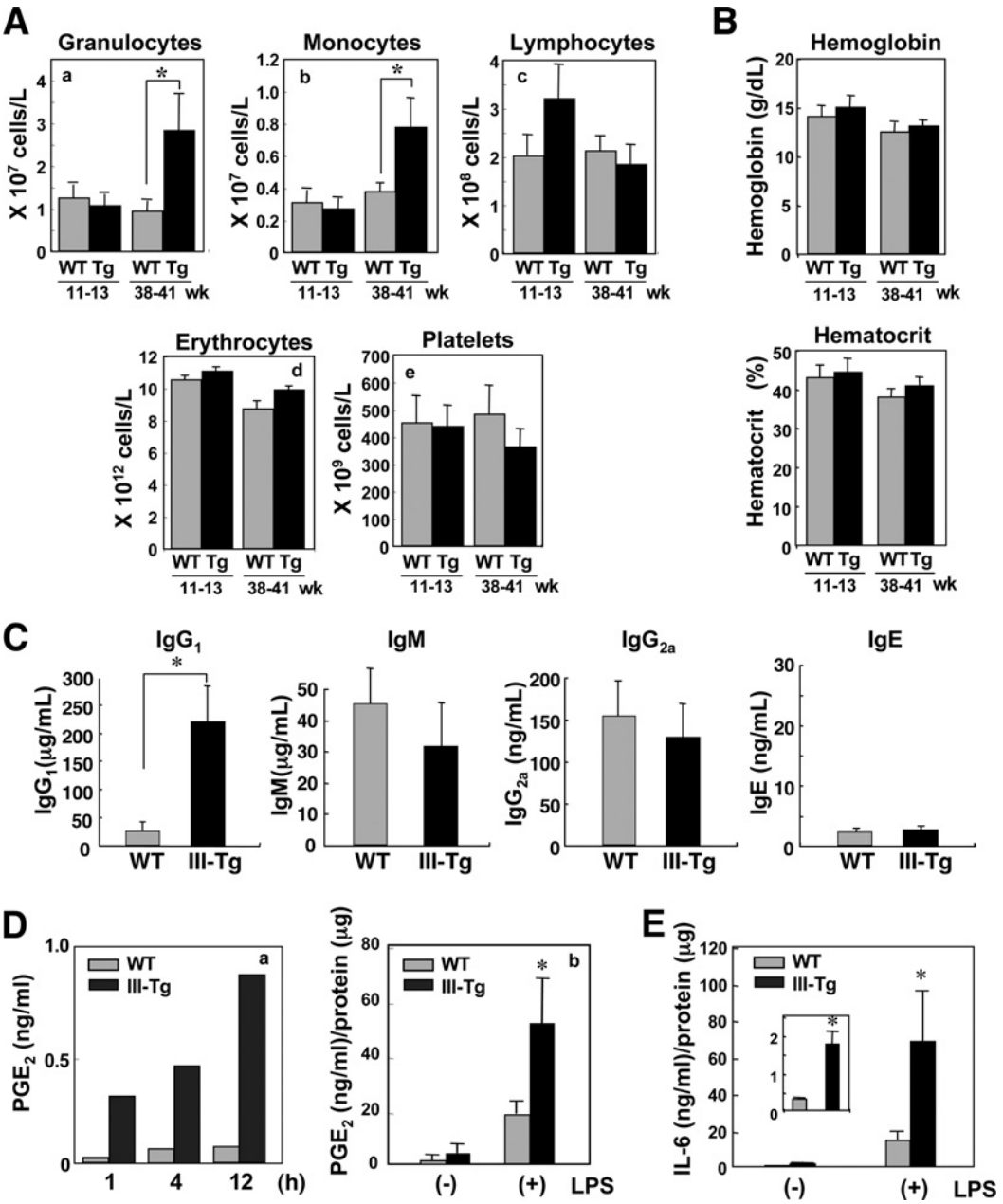

Figure 6 Changes in circulating cell populations and serum immunoglobulin levels in *Pla2g3*-Tg mice

The numbers of circulating granulocytes, monocytes, lymphocytes, platelets and erythrocytes (**A**), as well as haemoglobin and haematocrit values (**B**), in young (11–13-week-old) and aged (38–41-week-old) WT and *Pla2g3*-Tg (Tg) mice were evaluated using VetScan HM (means ± S.D., $n = 4$–12, $^*P < 0.05$). (**C**) Serum concentrations of IgG1, IgM, IgG2a and IgM were determined by sandwich ELISA (means ± S.D., $n = 3$, $^*P < 0.05$). (**D**) Peritoneal macrophages from *Pla2g3*-Tg (III-Tg) and WT mice were cultured for the indicated periods in culture medium (left-hand panel) or for 24 h in medium with (+) or without (−) 1 μg/ml LPS (right-hand panel). The supernatants were taken for PGE_2 enzyme immune assay. A representative result of two reproducible results (panel a) and means ± S.E.M. for four experiments (panel b) are shown. $^*P < 0.05$ compared with replicate WT cells. (**E**) Peritoneal macrophages from *Pla2g3*-Tg (III-Tg) and WT mice were cultured for 24 h in culture medium with (+) or without (−) LPS (right-hand panel). The supernatants were taken for ELISA for IL-6 (means ± S.E.M., $n = 4$, $^*P < 0.05$ compared with replicate WT cells). Inset, IL-6 production by the cells cultured in the absence of LPS is magnified.

in macrophages [24], a cell population which is increased in *Pla2g3*-Tg skin, and since its expression has been reported to be induced in cytokine-stimulated macrophage-like cells [25] and keratinocytes [26]. Increased expression of PLA2G2D has been reported in a mouse model of atopic dermatitis [27]. On the other hand, PLA2G2E and PLA2G2F, as well as endogenous PLA2G3, were consistently detected in WT and *Pla2g3*-Tg skin (Figure 3C), suggesting that these sPLA$_2$ enzymes are constitutively expressed in certain resident cells, rather than in infiltrating leucocytes, within the skin niche. Importantly, judging from the intensity of RT–PCR bands, the expression of endogenous mouse PLA2G3 in WT skin is similar to that of human PLA2G3 overexpressed in Tg skin (Figure 3C), suggesting a potential contribution of this enzyme to skin inflammation under certain pathological conditions. In contrast with previous reports describing the expression of PLA2G10 in newborn mouse skin [28], we failed to detect its transcript in the skin of either WT or *Pla2g3*-Tg mice (Figure 3C); this might be due to the difference in ages or strains

examined (neonatal NMRI mice compared with aged C57BL/6 mice).

As we have reported recently, alterations in plasma lipoproteins [a decrease in HDL (high-density lipoprotein) and an increase in atherogenic LDL (low-density lipoprotein)] occur in *Pla2g3*-Tg mice [16]. Interestingly, a potential linkage between altered lipoprotein levels and chronic inflammatory diseases has been proposed [29–32]. Mice deficient in LDL receptor and apolipoprotein A-I, in which plasma cholesterol levels were markedly altered, suffered from increasingly severe ulcerated cutaneous inflammation, and, in these mice, cholesterol accumulation in the skin was associated with macrophage infiltration and was accompanied by increases in TNFα and COX-2 [29,30]. Tg overexpression of apolipoprotein C1 decreased lipids in the sebaceous gland, epidermis and subcutaneous adipose tissue, leading to dry and scaly skin with loss of hair, epidermal hyperplasia, hyperkeratosis and atrophic sebaceous glands lacking sebum [31]. An increase in circulating HDL led to a significant inhibition of basal and IL-1α-induced E-selectin expression, suggesting the potential anti-inflammatory action of HDL [32]. These observations raise the possibility that systemic alterations in circulating LDL and HDL in *Pla2g3*-Tg mice [16] might be responsible, at least in part, for the acceleration of inflammation. Interestingly, *Pla2g2a*-Tg mice, which develop skin abnormalities [4], also show reduced plasma HDL levels [10], and disturbance of systemic lipid homoeostasis has often been linked with skin abnormalities in various mouse models and even in human diseases [33–35]. Therefore potential causal relationships between altered systemic lipoprotein levels and skin abnormalities in mouse models with Tg overexpression of particular forms of $sPLA_2$ should be taken into account. Moreover, given the recent recognition that atherosclerosis is a form of chronic inflammation in the vascular wall [36], the atherosclerotic [16] and inflammatory (the present study) phenotypes of *Pla2g3*-Tg mice may be interrelated.

Endogenous *PLA2G3* mRNA in humans is detected in several tissues such as kidney, heart, liver and skeletal muscle [13], and immunoreactive PLA2G3 protein is localized in microvascular endothelial cells, macrophages, peripheral neuronal fibres, atherosclerotic plaques and tumour cells in tissues from human subjects with diseases (e.g. inflammation, ischaemia, atherosclerosis and cancer) [15,16,37,38]. In mice, endogenous *Pla2g3* mRNA is detected at trace levels in various tissues (H. Sato, Y. Taketomi and M. Murakami, unpublished work), among which the nervous system (e.g. brain, spinal cord and dorsal root ganglion) shows the highest expression [37]. Essentially, unlike PLA2G2A, whose tissue expression profiles differ considerably between human and mouse [20], it appears that human and mouse PLA2G3 orthologues ($\sim$82% homology in their core S domain) display a similar, if not entirely identical, tissue distribution pattern. In cell culture systems, forcible expression or exogenous addition of human PLA2G3 facilitates the axonal growth and survival of neuronal cells, proliferation of colorectal cancer cells, maturation of dendritic cells, migration of endothelial cells and inhibition of viral infection, whereas introduction of PLA2G3-directed small interfering RNA partially suppresses some of these events, probably through altering the cellular levels of lysophospholipids or eicosanoids [14,15,37,39,40]. Detection of endogenous PLA2G3 in mouse skin (Figure 3C) raises the intriguing possibility that this unique type of $sPLA_2$ might function in skin biology. Besides the effect of PLA2G3 on lipid mediator generation, PLA2G3 might be coupled with a particular signalling pathway through interacting with the putative N-type $sPLA_2$ receptor, to which bee venom PLA_2 (a PLA2G3 homologue) is known to bind as a ligand [41]. It will be necessary to reconcile the precise *in vivo* actions, expression and dynamics of PLA2G3 by conducting studies with *Pla2g3* gene-disrupted mice or with PLA2G3-specific inhibitors. Nevertheless, despite the limitations of Tg overexpression strategies, the mouse model described in the present paper might be useful to uncover the molecular actions of $sPLA_2$ family enzymes, including tissue-specific target substrates and their metabolites, during the process of inflammation or other related diseases. Furthermore, this mouse line has potential for the screening of novel anti-inflammatory agents aiming at inhibiting $sPLA_2$-mediated phospholipid hydrolysis.

AUTHOR CONTRIBUTION

This paper was organized and written by Makoto Murakami. Most of the experiments, including maintenance of animals and preparation of samples, were performed by Hiroyasu Sato. Specifically, PCR analysis of $sPLA_2$s was assisted by Yoshitaka Taketomi, histochemistry by Seiko Masuda, experiments using peritoneal macrophages by Yuki Isogai and Tetsuyuki Kobayashi, and FACS analysis by Kei Yamamoto.

ACKNOWLEDGMENTS

We thank Dr Y. Ishikawa and Dr T. Ishii (Toho University, Tokyo, Japan) and Dr Y. Takanezawa (University of Tokyo, Tokyo, Japan) for their assistances for histological and ESI–MS analyses respectively.

FUNDING

This work was supported by grants-in-aid for scientific research from the Ministry of Education, Science, Culture, Sports and Technology of Japan [grant numbers 21390027, 21791106 and 21790093], Precursory Research for Embryonic Science and Technology (PRESTO) from the Japan Science and Technology Agency, the Tokyo Biochemical Research Foundation, the Mitsubishi Pharma Research Foundation, the Novartis Foundation for the Promotion of Science and the Takeda Science Foundation.

REFERENCES

1 Murakami, M. and Kudo, I. (2001) Diversity and regulatory functions of mammalian secretory phospholipase A_2s. Adv. Immunol. **77**, 163–194
2 Kudo, I. and Murakami, M. (2002) Phospholipase A_2 enzymes. Prostaglandins Other Lipid Mediat. **68–69**, 3–58
3 Lambeau, G. and Gelb, M. H. (2008) Biochemistry and physiology of mammalian secreted phospholipases A_2. Annu. Rev. Biochem. **77**, 495–520
4 Grass, D. S., Felkner, R. H., Chiang, M.-Y., Wallace, R. E., Nevalainen, T. J., Bennett, C. F. and Swanson, M. E. (1996) Expression of human group II PLA_2 in transgenic mice results in epidermal hyperplasia in the absence of inflammatory infiltrate. J. Clin. Invest. **97**, 2233–2241
5 Satake, Y., Diaz, B. L., Balestrieri, B., Lam, B. K., Kanaoka, Y., Grusby, M. J. and Arm, J. P. (2004) Role of group V phospholipase A_2 in zymosan-induced eicosanoid generation and vascular permeability revealed by targeted gene disruption. J. Biol. Chem. **279**, 16488–16494
6 Muñoz, N. M., Meliton, A. Y., Arm, J. P., Bonventre, J. V., Cho, W. and Leff, A. R. (2007) Deletion of secretory group V phospholipase A_2 attenuates cell migration and airway hyperresponsiveness in immunosensitized mice. J. Immunol. **179**, 4800–4807
7 Fujioka, D., Saito, Y., Kobayashi, T., Yano, T., Tezuka, H., Ishimoto, Y., Suzuki, N., Yokota, Y., Nakayama, T., Obata, J. E. et al. (2008) Reduction in myocardial ischemia/reperfusion injury in group X secretory phospholipase A_2-deficient mice. Circulation **117**, 2977–2985
8 Henderson, Jr, W. R., Chi, E. Y., Bollinger, J. G., Tien, Y. T., Ye, X., Castelli, L., Rubtsov, Y. P., Singer, A. G., Chiang, G. K., Nevalainen, T. et al. (2007) Importance of group X-secreted phospholipase A_2 in allergen-induced airway inflammation and remodeling in a mouse asthma model. J. Exp. Med. **204**, 865–877
9 Laine, V. J., Grass, D. S. and Nevalainen, T. J. (1999) Protection by group II phospholipase A_2 against *Staphylococcus aureus*. J. Immunol. **162**, 7402–7408
10 Ivandic, B., Castellani, L. W., Wang, X. P., Qiao, J. H., Mehrabian, M., Navab, M., Fogelman, A. M., Grass, D. S., Swanson, M. E., de Beer, M. C. et al. (1999) Role of group II secretory phospholipase A_2 in atherosclerosis. 1. Increased atherogenesis and altered lipoproteins in transgenic mice expressing group IIa phospholipase A_2. Arterioscler. Thromb. Vasc. Biol. **19**, 1284–1290

11 Ohtsuki, M., Taketomi, Y., Arata, S., Masuda, S., Ishikawa, Y., Ishii, T., Takanezawa, Y., Aoki, J., Arai, H., Yamamoto, K. et al. (2006) Transgenic expression of group V, but not group X, secreted phospholipase A_2 in mice leads to neonatal lethality because of lung dysfunction. J. Biol. Chem. **281**, 36420–36433

12 Curfs, D. M. J., Ghequiere, S. A. I., Vergouwe, M. N., van der Made, I., Gijbels, M. J. J., Greaves, D. R., Verbeek, J. S., Hofker, M. H. and de Winther, M. P. J. (2008) Macrophage secretory phospholipase A_2 group X enhances anti-inflammatory responses, promotes lipid accumulation, and contributes to aberrant lung pathology. J. Biol. Chem. **283**, 21640–21648

13 Valentin, E., Ghomashchi, F., Gelb, M. H., Lazdunski, M. and Lambeau, G. (2000) Novel human secreted phospholipase A_2 with homology to the group III bee venom enzyme. J. Biol. Chem. **275**, 7492–7496

14 Murakami, M., Masuda, S., Shimbara, S., Bezzine, S., Ladzunski, M., Lambeau, G., Gelb, M. H., Matsukura, S., Kokubu, F., Adachi, M. and Kudo, I. (2003) Cellular arachidonate-releasing function of novel classes of secretory phospholipase A_2s (group III and XII). J. Biol. Chem. **278**, 10657–10667

15 Murakami, M., Masuda, S., Shimbara, S., Ishikawa, Y., Ishii, T. and Kudo, I. (2005) Cellular distribution, post-translational modification, and tumorigenic potential of human group III secreted phospholipase A_2. J. Biol. Chem. **280**, 24987–24998

16 Sato, H., Kato, R., Isogai, Y., Saka, G., Ohtsuki, M., Taketomi, Y., Yamamoto, K., Tsutsumi, K., Yamada, J., Masuda, S. et al. (2008) Analyses of group III secreted phospholipase A_2 transgenic mice reveals potential participation of this enzyme in plasma lipoprotein modification, macrophage foam cell formation, and atherosclerosis. J. Biol. Chem. **283**, 33483–33497

16a Bligh, E. G. and Dyer, W. J. (1959) A rapid method of total lipid extraction and purification. J. Biochem. Physiol. **37**, 911–917

17 Ghosh, A. K., Hirasawa, N., Ohtsu, H., Watanabe, T. and Ohuchi, K. (2002) Defective angiogenesis in the inflammatory granulation tissue in histidine decarboxylase-deficient mice but not in mast cell-deficient mice. J. Exp. Med. **195**, 973–982

18 Murakami, M., Naraba, H., Tanioka, T., Semmyo, N., Nakatani, Y., Kojima, F., Ikeda, T., Fueki, M., Ueno, A., Oh-Ishi, S. and Kudo, I. (2000) Regulation of prostaglandin E_2 biosynthesis by inducible membrane-associated prostaglandin E_2 synthase that acts in concert with cyclooxygenase-2. J. Biol. Chem. **275**, 32783–32792

19 Uozumi, N., Kume, K., Nagase, T., Nakatani, N., Ishii, S., Tashiro, F., Komagata, Y., Maki, K., Ikuta, K., Ouchi, Y. et al. (1997) Role of cytosolic phospholipase A_2 in allergic response and parturition. Nature **390**, 618–622

20 MacPhee, M., Chepenik, K. P., Liddell, R. A., Nelson, K. K., Siracusa, L. D. and Buchberg, A. M. (1995) The secretory phospholipase A_2 gene is a candidate for the *Mom1* locus, a major modifier of *Apc^{Min}*-induced intestinal neoplasia. Cell **81**, 957–966

21 Mulherkar, R., Kirtane, B.M., Ramchandani, A., Mansukhani, N.P., Kannan, S. and Naresh, K.N. (2003) Expression of enhancing factor/phospholipase A_2 in skin results in abnormal epidermis and increased sensitivity to chemical carcinogenesis. Oncogene **22**, 1936–1944

22 Murakami, M., Kambe, T., Shimbara, S., Higashino, K., Hanasaki, K., Arita, H, Horiguchi, M., Arita, M., Arai, H., Inoue, K. and Kudo, I. (1999) Different functional aspects of the group II subfamily (types IIA and V) and type X secretory phospholipase A_2s in regulating arachidonic acid release and prostaglandin generation. J. Biol. Chem. **274**, 31435–31444

23 Masuda, S., Murakami, M., Takanezawa, Y., Aoki, J., Arai, H., Ishikawa, Y., Ishii, T., Arioka, M. and Kudo, I. (2005) Neuronal expression and neuritogenic action of group X secreted phospholipase A_2. J. Biol. Chem. **280**, 23203–23214

23a Sung, Y. M., He, G., Hwang, D. H. and Fischer, S. M. (2006) Overexpression of the prostaglandin E_2 receptor EP2 results in enhanced skin tumor development. Oncogene **25**, 5507–5516

24 Balestrieri, B., Hsu, V. W., Gilbert, H., Leslie, C. C., Han, W. K., Bonventre, J. V. and Arm, J. P. (2006) Group V secretory phospholipase A_2 translocates to the phagosome after zymosan stimulation of mouse peritoneal macrophages and regulates phagocytosis. J. Biol. Chem. **281**, 6691–6698

25 Balboa, M. A., Balsinde, J., Winstead, M. V., Tischfield, J. A. and Dennis, E. A. (1996) Novel group V phospholipase A_2 involved in arachidonic acid mobilization in murine P388D1 macrophages. J. Biol. Chem. **271**, 32381–32384

26 Rys-Sikora, K. E., Konger, R. L., Schoggins, J. W., Malaviya, R. and Pentland, A. P. (2000) Coordinate expression of secretory phospholipase A_2 and cyclooxygenase-2 in activated human keratinocytes. Am. J. Physiol. Cell. Physiol. **278**, C822–C833

27 Murakami, M., Yoshihara, K., Shimbara, S., Sawada, M., Inagaki, N., Nagai, H., Naito, M., Tsuruo, T., Moon, T. C., Chang, H. W. and Kudo, I. (2002) Group IID heparin-binding secretory phospholipase A_2 is expressed in human colon carcinoma cells and human mast cells and upregulated in mouse inflammatory tissues. Eur. J. Biochem. **269**, 2698–2707

28 Hass, U., Podda, M., Behne, M., Gurrieri, S., Alonso, A., Fürstenberger, G., Pfeilschifter, J., Lambeau, G., Gelb, M. H. and Kaszkin, M. (2005) Characterization and differentiation-dependent regulation of secreted phospholipase A_2 in human keratinocytes and in healthy and psoriatic human skin. J. Invest. Dermatol. **124**, 204–211

29 Zabalawi, M., Bhat, S., Loughlin, T., Thomas, M. J., Alexander, E., Cline, M., Bullock, B., Willingham, M. and Sorci-Thomas, M. G. (2003) Induction of fatal inflammation in LDL receptor and ApoA-I double-knockout mice fed dietary fat and cholesterol. Am. J. Pathol. **163**, 1201–1213

30 Zabalawi, M., Bharadwaj, M., Horton, H., Cline, M., Willingham, M., Thomas, M. J. and Sorci-Thomas, M. G. (2007) Inflammation and skin cholesterol in *LDLr$^{-/-}$*, *apoA-I$^{-/-}$* mice: link between cholesterol homeostasis and self-tolerance? J. Lipid Res. **48**, 52–65

31 Jong, M. C., Gijbels, M. J., Dahlmans, V. E., Gorp, P. J., Koopman, S. J., Ponec, M., Hofker, M. H. and Havekes, L. M. (1998) Hyperlipidemia and cutaneous abnormalities in transgenic mice overexpressing human apolipoprotein C1. J. Clin. Invest. **101**, 145–152

32 Cockerill, G. W., Huehns, T. Y., Weerasinghe, A., Stocker, C., Lerch, P. G., Miller, N. E. and Haskard, D. O. (2001) Elevation of plasma high-density lipoprotein concentration reduces interleukin-1-induced expression of E-selectin in an *in vivo* model of acute inflammation. Circulation **103**, 108–112

33 Weserberg, R., Tvrdik, P., Undén, A.-B., Månsson, J.-E., Norlén, L., Jakobsson, A., Holleran, W. H., Elias, P. M., Asadi, A., Flodby, P. et al. (2004) Role for ELOVL3 and fatty acid chain length in development of hair and skin function. J. Biol. Chem. **279**, 5621–5629

34 Zheng, Y., Eilertsen, K. J., Ge, L., Zhang, L., Sundberg, J. P., Prouty, S. M., Stenn, K. S. and Parimoo, S. (1999) Scd1 is expressed in sebaceous glands and is disrupted in the *asebia* mouse. Nat. Genet. **23**, 268–270

35 Stone, S. J., Myers, H. M., Watkins, S. M., Brown, B. E., Feingold, K. R., Elias, P. M. and Farese, Jr, R. V. (2004) Lipopenia and skin barrier abnormalities in DGAT2-deficient mice. J. Biol. Chem. **279**, 11767–11776

36 Libby, P. (2002) Inflammation in atherosclerosis. Nature **420**, 868–874

37 Masuda, S., Yamamoto, K., Hirabayashi, T., Ishikawa, Y., Ishii, T., Kudo, I. and Murakami, M. (2008) Human group III secreted phospholipase A_2 promotes neuronal outgrowth and survival. Biochem. J. **409**, 429–438

38 Mounier, C. M., Wendum, D., Greenspan, E., Fléjou, J. F., Rosenberg, D. W. and Lambeau, G. (2008) Distinct expression pattern of the full set of secreted phospholipases A_2 in human colorectal adenocarcinomas: sPLA$_2$-III as a biomarker candidate. Br. J. Cancer **98**, 587–595

39 Perrin-Cocon, L., Agaugué, S., Coutant, F., Masurel, A., Bezzine, S., Lambeau, G., André, P. and Lotteau, V. (2004) Secretory phospholipase A_2 induces dendritic cell maturation. Eur. J. Immunol. **34**, 2293–2302

40 Mitsuishi, M., Masuda, S., Kudo, I. and Murakami, M. (2007) Human Group III phospholipase A_2 suppresses adenovirus infection into host cells: evidence that group III, V and X phospholipase A_2s act on distinct cellular phospholipids molecular species. Biochim. Biophys. Acta **1771**, 1389–1396

41 Nicolas, J. P., Lin, Y., Lambeau, G., Ghomashchi, F., Lazdunski, M. and Gelb, M. H. (1997) Localization of structural elements of bee venom phospholipase A_2 involved in N-type receptor binding and neurotoxicity. J. Biol. Chem. **272**, 7173–7181

Received 23 December 2008/9 March 2009; accepted 17 April 2009
Published as BJ Immediate Publication 17 April 2009, doi:10.1042/BJ20082429